Micro-scale Testing to Evaluate the Fracture Characteristics of Quasi-brittle Materials

<u>Dong Liu</u>[1,2*], Peter Heard[1] and Peter E J Flewitt[1,3]

[1]Interface Analysis Centre, University of Bristol, Bristol, BS2 8BS, UK
[2]Department of Mechanical Engineering, University of Bristol, Bristol, BS8 1TR, UK
[3]School of Physics, HH Wills Laboratory, University of Bristol, Bristol, BS8 1TL,
* Corresponding author: dong.liu@bristol.ac.uk

Abstract   In this paper micro-scale testing techniques have been implemented on two types of quasi-brittle material: pile grade A (PGA) graphite and air-plasma sprayed yttria (7 wt.%) stabilized zirconia (APS-YSZ). One approach uses a force measurement system within a FEI Helios Dualbeam FIB/SEM workstation, which allows the fracture characteristics and mechanical properties of the two materials to be evaluated and correlated with local microstructural features. In addition for PGA graphite, disc-compression and trench-probe methods have been applied. Hence the initiation, propagation of the cracks and the corresponding deformation can be recorded and investigated. For the APS-YSZ, micro-scale cantilevers have been fabricated using FIB and a load-recording probe has been applied in-situ. The fracture toughness, flexural strength and the cracking path are analysed. Interpretation of these tests has contributed to the understanding of the macro-scale quasi-brittle mechanical behaviour of the two materials.

Keywords   Pile grade A graphite, Air-plasma-sprayed yttria stabilized zirconia, Disc compression, Micro-scale cantilever testing

1. Introduction

Pile Grade A (PGA) graphite used for a wide range of applications, including nuclear reactor core, is often cited as a classic example of a brittle material because failure, in tension, is associated with small strains. It has been recognised that these graphites are multiphase, polygranular, aggregate structures and have features similar to other aggregate materials such as concrete [1, 2]. However, attempts to characterise the fracture behaviour of graphite by linear elastic fracture mechanics methods have been largely unsuccessful. Observations of graphite fracture show that elastic strain energy may be dissipated by the formation of distributed micro-cracks and their formation may be responsible for non-linearity in the rising load-displacement curve [3, 4]. A typical example is shown by the load-displacement response for bend geometry specimens, Fig. 1. There is no evidence that polygranular, aggregate graphites can be plastically deformed. Hence, the change in compliance together with any deviation from an initial linear shape of the load-displacement curve, Region II in Fig. 1, can be attributed to micro-cracking. Progressive softening is also observed in some specimens post the peak load, Region III. This type of load-displacement behaviour is a characteristic of quasi-brittle materials [2]. Air-plasma-sprayed (APS) yttria (7 wt.%) stabilized zirconia (YSZ) has been applied widely in thermal barrier coating systems (TBC) to isolate metallic components from the high temperature environmental gas in crucial parts of engines. APS produces TBC with a splat microstructure, moderate porosity and compliance, and low thermal conductivity. For example, APS-YSZ coatings on turbine blades are normally 150 to 300 μm thick sustaining a temperature difference up to 300 °C. Due to manufacturing, the APS-YSZ splat microstructure contains defects, pores and unmelted particles. These internal microstructures result in non-linear brittle behaviour of the coatings.

To understand the macro-scale mechanical behaviour of these types of quasi-brittle materials, micro-scale testing samples an appropriate small volume of material and localised microstructure to characterise initiation and propagation of micro-cracks. This paper considers micro-scale tests undertaken by the research group at the University of Bristol, UK [2, 4-6].
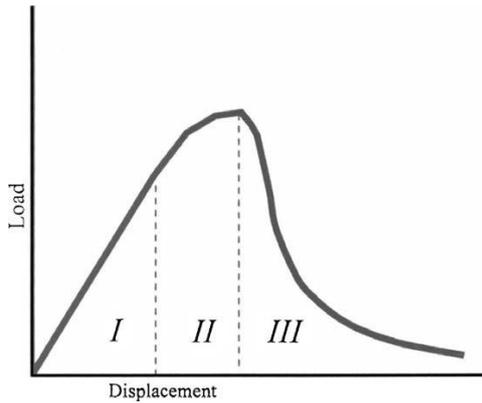
Fig.1 A characteristic bend geometry load-displacement curve for a quasi-brittle material, region I is linear, region II is non-linear, region III is post peak softening.

2. Experiments

2.1. Materials

Cylindrical PGA test specimens were made by trepanning 12 mm diameter rods extracted from bulk virgin PGA graphite reactor core bricks. These were sliced into 6 mm thick cylinders using a South Bay Technology Inc. Model 650 low speed diamond wheel saw with deionised water as coolant. The diamond saw produced smooth high-quality surfaces suitable for subsequent microscopic examination. The brick extrusion direction was diametrically across the flat surfaces of the cut cylinders. The extrusion direction was marked on the edges of the cylinders for reference during compression testing.

For testing of APS-YSZ specimens, samples manufactured by Praxair Surface Technologies Ltd with a curved geometry designed to simulate key features of coated blade were used. Each comprised a Superalloy substrate (CMSX4) with air plasma sprayed (APS) 7 wt.% Y_2O_3-stabilised ZrO_2 (YSZ) applied onto an Amdry 995 bond coat deposited using high velocity oxygen fuel (HVOF) [7]. The thickness of the TBC varied with position around the specimen from 130 µm to 230 µm. A typical cross-section of the TBC system is shown in Fig. 2a. The YSZ which is ~200 µm thick comprises lameller splats, micro-scale air pores and defects. The interfaces, YSZ-TBC/TGO and TGO/BC, are undulating with a variable thickness of TGO. In this present work, the focus was on the APS-YSZ material in as-coated condition, and the specimens are tapered to reveal the interfaces, Fig. 2b. Micro-cantilever specimens with the size of ~2×2×10 µm are created at preferred locations of this coating as shown in Fig. 2b.
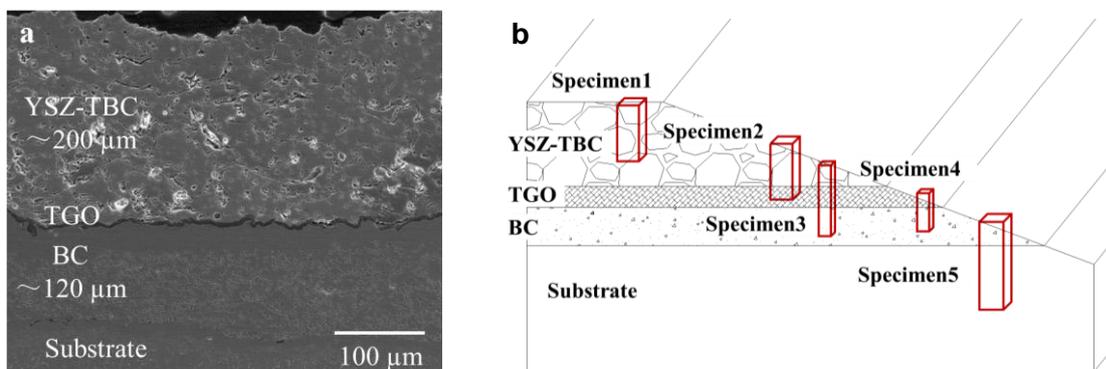

Fig. 2 The TBC system (a) typical cross-section for specimen that has been oxidised for 100 hours at 925°C and (b) creation of micro-cantilever specimen at preferred locations on tapered surface.

2.2 Testing methods

Controlled cracking was introduced in the quasi-brittle specimens using appropriate methods. Each method allowed specimens to be subsequently examined under load.

2.2.1 Disc compression method

Compression testing of the cylindrical graphite specimens was done using a Deben compression/tensile stage (MicroTest 2000 model, Gatan Ltd., Abingdon, Oxon, UK), Fig. 3. The unit is capable of operation externally or within a scanning electron microscope or focused ion beam (FIB) workstation. The stage can be operated at compression speeds of between 0.033 and 0.4 mm/min, with a load cell giving force measurements up to a maximum of 2 kN. The cylindrical graphite specimens were loaded into the compression tester such that the direction of the compressive load was along a diameter of the flat face of the cylinders, chosen here to be the extrusion direction of the graphite. This provided a tensile load normal to the direction of the applied load so that cracks would be induced in the plane parallel to the load direction. Load-displacement curves were recorded whilst observing the surface of the specimen by optical microscopy or focused ion beam imaging.
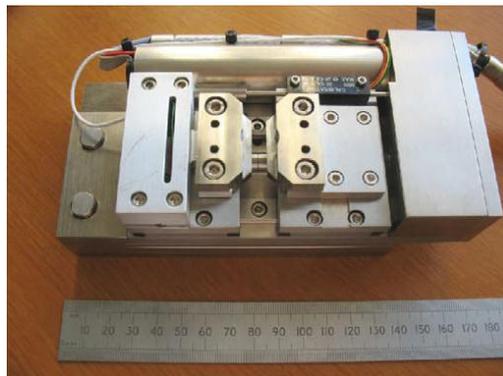

Fig. 3 Compression tester applied in micro-scale mechanical testing.
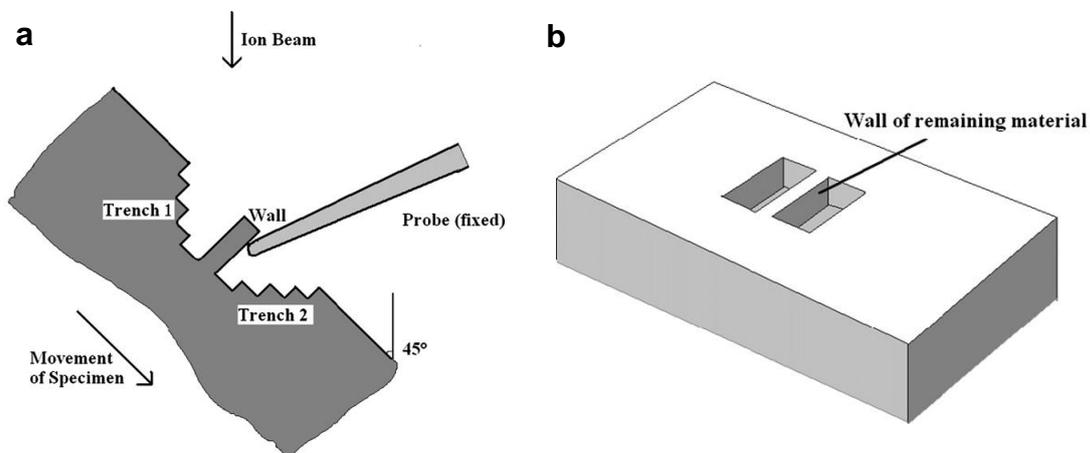
2.2.2 Trench-probe loading method

Fig. 4 (a) Schematic of the trench-probe method for applying a force to a prepared wall of material 35 μm long within the FIB; (b) the thin wall of residual materials created between the two trenches.

The trench-probe method provided a means of applying a small, progressive, localised force to a prepared region of a 'wall' specimen of graphite whilst it was under observation in the FIB workstation, Fig. 4. For this, a sharpened steel probe (tip radius 5 μm approximately) was attached to the end of a spare gas injector on the instrument. The retractable probe was aligned to be in the centre of the field of view, so that it could be used to push on a prepared part of the specimen, Fig. 4a. Local deformation and cracking could be studied at high resolution within chosen regions of a specimen, Fig. 4b.

2.2.3 Micro-cantilever beam bending method

The experimental arrangement for the mechanical property testing was a combination of a FEI Helios NanoLab 600i Dualbeam workstation and a compact force measurement system supplied by Kleindiek which allowed in-situ loading and force readout, Fig. 5a. The dualbeam workstation provided ion beam milling and in-situ SEM imaging. Before commencing the measurements, a calibration of the force sensor was carried out by loading a standard spring embedded in the system to provide the resistance conversion references and zero the load reading. Details of the force measurement system and the cantilever specimen preparation are described elsewhere [8, 9]. A typical set up of in-situ loading of a cantilever beam using the force measurement probe is shown in Fig. 5b.
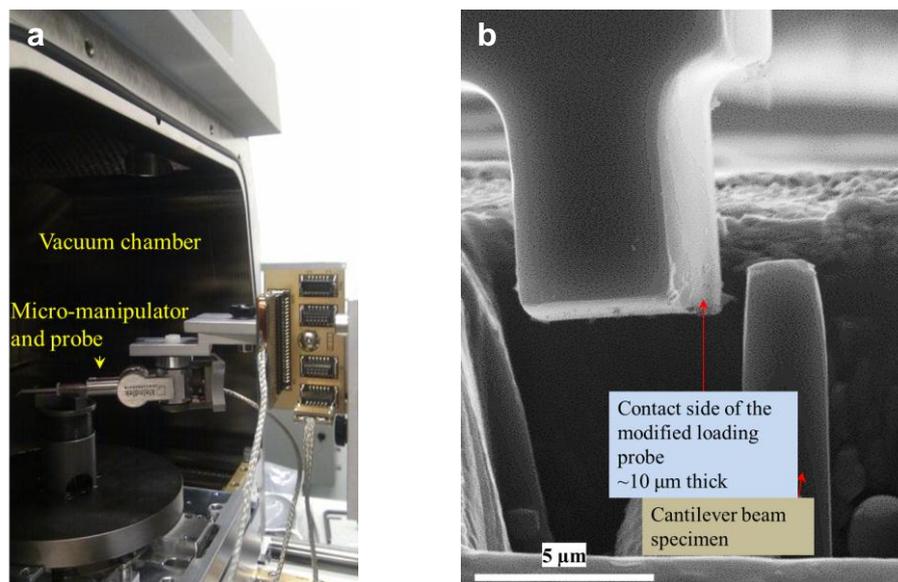

Fig. 5 (a) Installation of the FMS into the dualbeam FIB vacuum chamber. Side-view showing the FMS in the middle of the stage (b) SEM image showing loading the micro-cantilever specimen.

3. Results

3.1 Load and displacement

3.1.1 PGA graphite in compression

PGA graphite has a complex structure of filler particles interspersed within a matrix which consists of small flour particles and the graphitised pitch together with porosity. When examined at high resolution in the FIB, the two areas have very distinct microstructures. Filler particles (Fig. 6a left hand side) are solid with isolated shrinkage (Mrozowski) cracks. The matrix areas (Fig. 6a right hand side) are dominated by the presence of lamellar graphite. This is believed to be the graphite residue of the mesophase produced during the graphitisation of the pitch. Serial sections of the

region shown in Fig. 6a and in other similar areas reveal that the porosity in such regions is interconnected.

The load-displacement curve resulting from compression of a cylindrical PGA specimen is shown in Fig. 6b. Compression proceeded at a rate of 0.1 mm/min. Displacement and load measurements were recorded at 500 ms intervals. The initial region, up to 0.1 mm displacement, had a relatively low slope, characteristic of a "bedding-in" region in which the specimen accommodated to the compression clamps. A linear region was observed between 0.2 and 0.3 mm displacement, in which elastic deformation occurred. Beyond this point the curve became non-linear with a gradually reducing compliance, until peak force was reached. After the maximum force, failure was gradual with force reducing slowly with displacement.
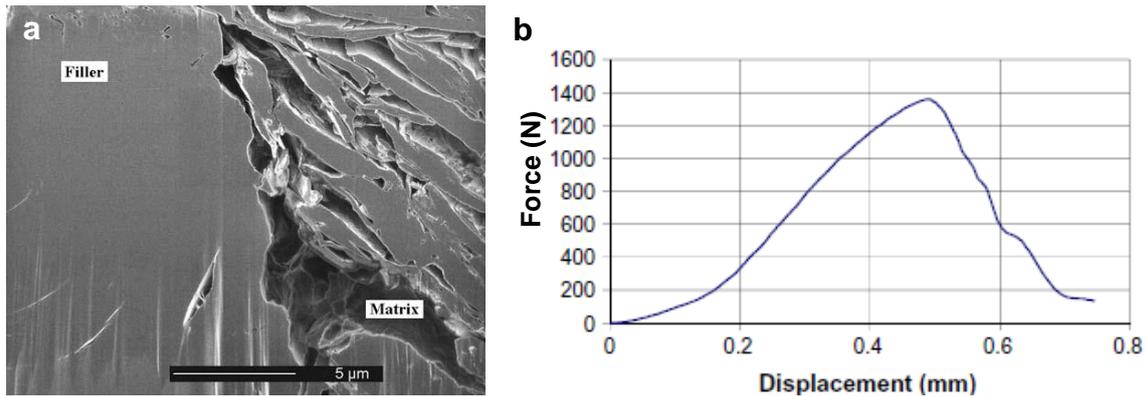

Fig. 6 (a) Microstructure of virgin PGA graphite revealed by FIB sectioning and imaging; (b) Load-displacement curve from compression of a cylindrical PGA specimen.
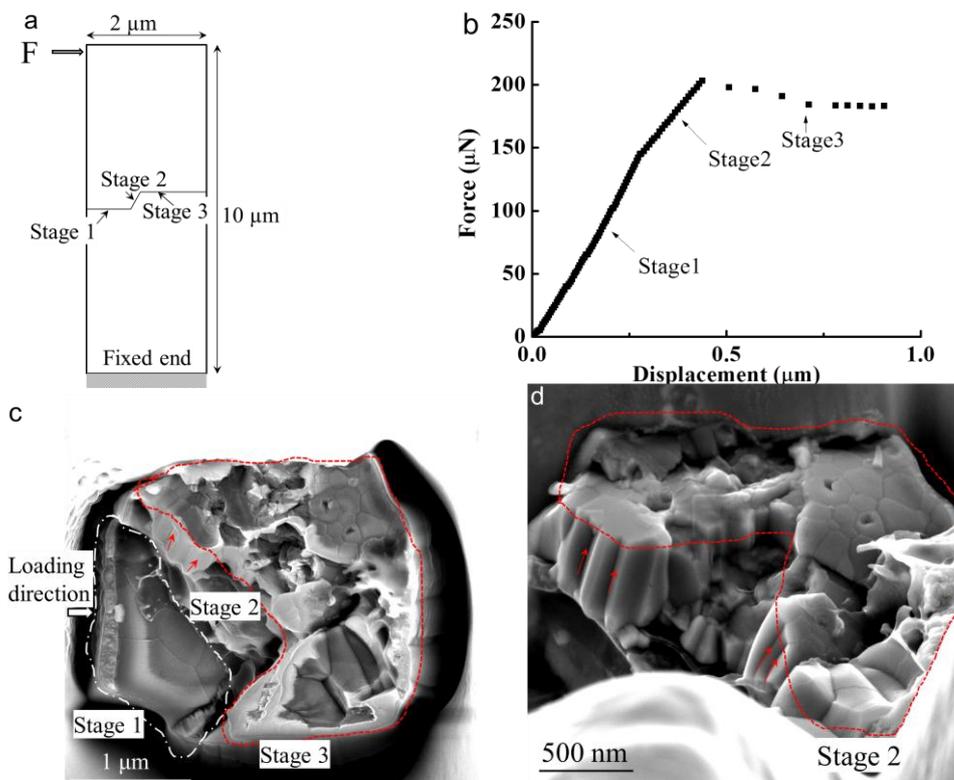

Fig. 7 A cantilever specimen containing a surface breaking flaw. (a) Schematic of the loaded specimen. (b) Force-deflection curve. (c) Surface of brittle fracture (the arrow indicates the load direction). (d) Side view of the fractured surface revealing vertical steps along the grains [6].

3.1.2 APS-YSZ in bending

In the case of a typical cantilever specimen, the force-deflection curve, Fig. 7b, containd three distinct stages 1 to 3. During stage 1 there was elastic deflection and at the end of this stage (~150 µN) the gradient changed. Stage 2 reached a maximum at ~200 µN. This was followed by a period of stable deflection as cracks propagated during stage 3. Examination of the final fracture surface, Fig. 7c, revealed the initial pre-existing flaw. There was evidence for some crack extension during stage 2 and then mainly inter-granular brittle fracture in stage 3, Fig. 7d. The elastic modulus calculated from the first linear part of the loading curve gave a value of ~35±5 GPa which is within the range of macroscopic values of 10 to 100 GPa [10-13]. Fracture toughness can be derived from the maximum load to be ~ 5.30 MPa·m$^{1/2}$ which is at the higher end of the macroscopic range of values, 0.7 to 5 MPa·m$^{1/2}$ [14-16].

3.2 Crack initiation and propagation

3.2.1 Disc compression

The compression method was used on a PGA graphite specimen within the FIB work station. Compression proceeded until fine cracking was observed at a pre-peak load at the top surface of the specimen. Sites were then chosen for FIB trenching, generally at positions across the observed cracks close to the crack tip, or ahead of the crack tip. The specimen was then tilted to 45° for high-resolution imaging of the cut face to observe sub-surface detail. Compression was resumed, increasing the load by small increments, realigning the specimen to centre the region of interest in the field of view and recording images. Force increments of 40 N were used and FIB images were captured at 8000× magnification, giving a horizontal field of view of 38 µm. Fig. 8 shows, optical images Fig. 8a and b and FIB images Fig. 8c and d, of the cut face of the specimen at compression loads of: (c) 497 N, and (d) 830 N respectively. The arrows in Figs. 8c and d mark the position of a crack forming and developing in the bulk of the graphite, within a filler particle. After crack formation, the two halves slide across each other.
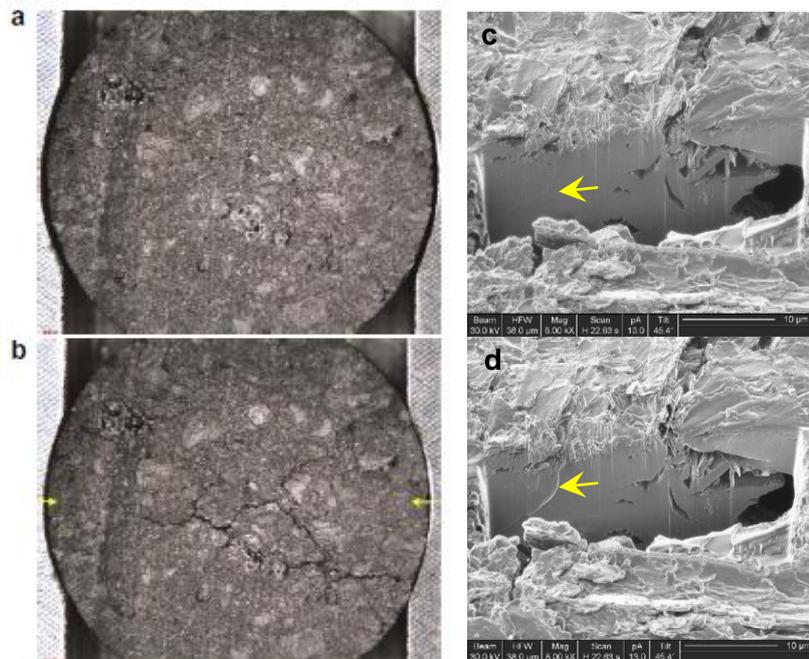

Fig. 8 Optical image of PGA specimen: (a) before compression and (b) after 0.55 mm compressive displacement showing macro-cracking (displacement is horizontal, as shown by arrows). FIB images of PGA specimen under (c) 560 N and (d) 830 N compression. Arrows show developing micro-crack.
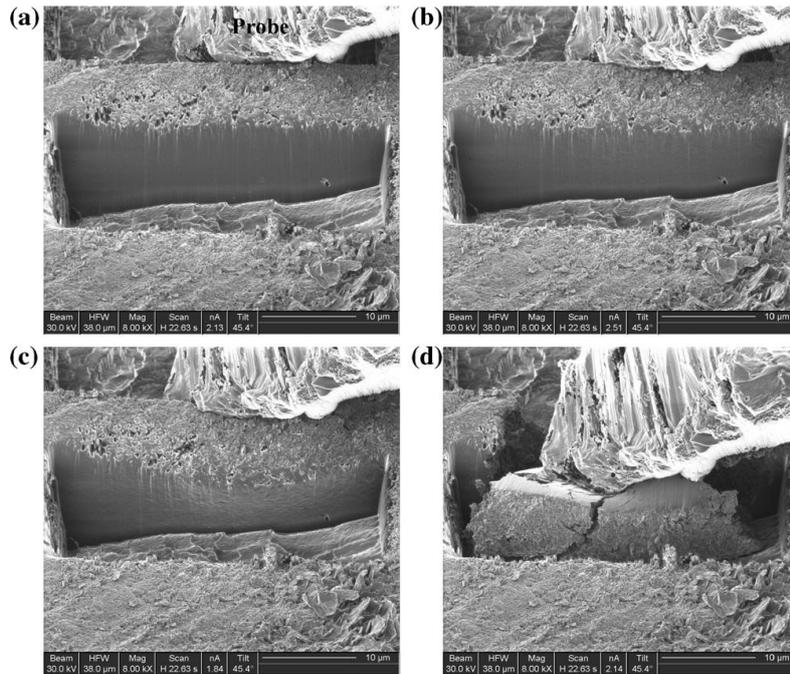
Fig. 9 Deformation of virgin PGA graphite filler using the trench-probe method. (a) Prior to loading (probe marked). (b) Showing onset of texturing. (c) Just prior to failure. (d) Just after failure.

3.2.3 Trench probe method

The trench-probe method was used to study the cracking of the individual components of the graphite microstructure such as filler particles or matrix. The method was used first on a virgin PGA specimen. Fig. 9 shows a sequence of FIB images of a region containing a filler particle recorded during testing. Fine undulations appeared at the cut surface of the specimen as it deformed, Fig. 9b, similar to those previously observed in deformed graphite. Failure occurred suddenly after considerable deformation, Fig. 9c, and the rapid movement of the probe at failure indicated that significant energy had been stored in the probe during deformation, which was released upon failure. In this case cracks formed at the mid position and ends of the loaded wall micro-specimen, Fig. 9d. The crack path was irregular and branched. Further measurements were undertaken on radiolytically oxidised PGA where twinning was observed and the cracking pattern was modified by the increase porosity within the material [5].

3.2.4 Micro-scale cantilever bending

Fig. 10a showed a typical cantilever beam created in APS-YSZ with a pre-existed external flaw (~0.1 μm) which is visible at one end of the splat boundary. The top of the beam is ~2 μm × 2 μm and a slight taper is present so that the base of the beam is ~2.2 μm × 2.2 μm. The force-deflection curve is shown in Fig. 10b and fracture occurred when the force reached ~301 μN. The fractured surface revealed an amorphous phase at the splat boundary which was in contact with the upper half of the beam before fracture, Fig. 10c. A detailed check of the fractured surface gave an equivalent crack area of 2 μm ×1 μm. In this figure, the large grains of YSZ (~0.8 μm in length) could be observed which were different from the upper side of the beam, where there were grains of sub-micrometre size. The tensile stress at fracture was ~3.6 GPa, and the elastic modulus of this particular beam was calculated to be ~43 GPa [6].
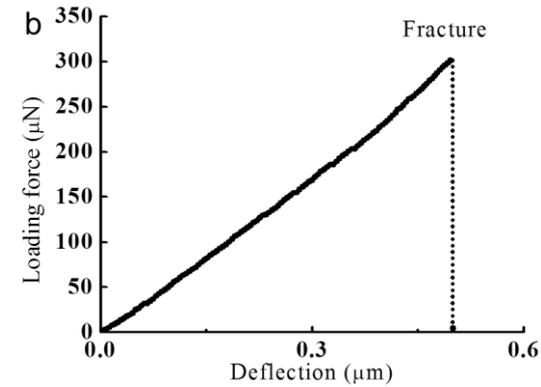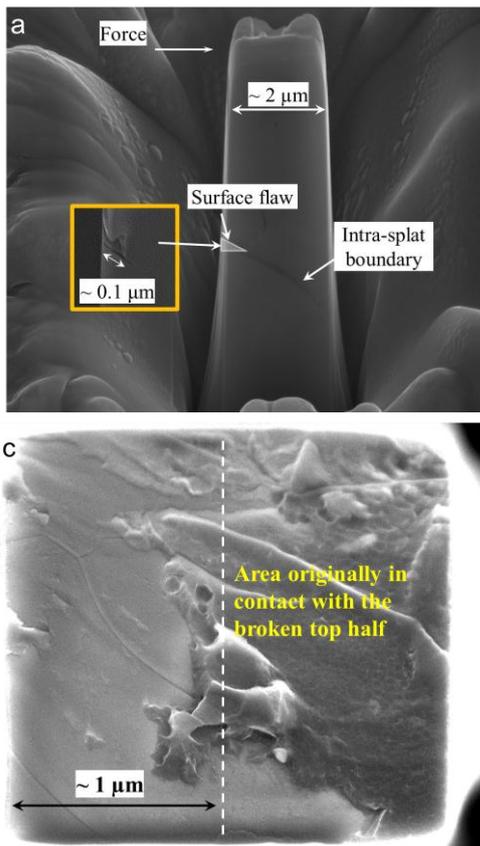
Fig. 10 A specimen created within APS-TBC. (a) Dimensions and a pre-existing flaw on the side of the cantilever with a size of ~0.1 μm as shown in insert. (b) Force-deflection curve. (c) Microstructure, dimensions of the fractured surface and the area which was in contact with the top half of the cantilever.

4. Discussion

Despite the widespread use of polygranular graphite for example for the construction of the gas cooled reactor cores in the UK reactor plant, there remain issues relating to the detailed understanding of the fracture processes at the micro-scale. Similar issues are associated with APS-YSZ as thermal barrier coatings. Here, the range of mechanical test methods assisted with understanding of the micro-scale mechanical fracture behaviour of these quasi-brittle materials.

The load-displacement curve, Fig. 6b, obtained for the compression disc test showed initial 'bedding' of the specimen to a load of about 300 N. There followed a short linear range where the material behaved elastically, prior to the onset of non-linearity. The ion milled section sequence, Figs. 8c and d, showed that as the load was increased to 560 N, Fig. 8c, a micro-crack formed and the feature became enhanced when the load reached 830 N, Fig. 8d. This sequence provides evidence that micro-cracks initiate and propagate prior to peak load to accommodate specimen displacement. At peak load and beyond, micro-cracks link to form the dominant macro-cracks shown in Fig. 6. Moreover Figs. 9a and 9b provided limited evidence for micro-cracking on the flank of a macro-crack. When interrupted post peak load, Figs. 9c and 9d showed that the macro-cracks follow an irregular path similar to that observed previously in the flexural test specimens of fractured un-irradiated PGA graphite [4]. The macro-cracks follow a path dominated by the direction of the applied tensile stress and the microstructure.

Two novel test procedures have been adopted to load graphite specimens combined with high-resolution imaging to investigate further the micro-cracking pre-peak load and macrocracking post peak load with respect to the microstructure of unirradiated PGA graphite. The disc compression test method provides the capability to view the surface of the small disc specimens when subject to a given load and under a progressively increasing applied load. The former is

important since, when using X-ray tomographic imaging of loaded and cracked, notched compact geometry unirradiated Gilsocarbon graphite specimens, Hodgkins et al. [3] observed closure of both the micro-and macro-cracks when the load was removed. This makes examination of cracking extremely difficult even when using high-resolution imaging techniques, for example focused ion beam imaging, unless a load is applied. The use of ion beam milling to produce surfaces normal to the specimen surface has provided the opportunity, for both test methods, to correlate surface and sub-surface microstructure and crack morphology. Fig. 6a provides a measure of the quality of such a milled surface in un-irradiated graphite.

One of the advantages of the in-situ micro-scale cantilever testing approach is the ability to record the specimen image at high resolution continually throughout the entire loading process. This enables the deflection of the cantilever at the loaded point to be captured and measured at the same time as the incremental loading force. This feature is especially important in the case of APS-TBC with its heterogeneous microstructure where the connecting ligaments fail. If the mechanical properties of these local ligaments can be mapped and incorporated into finite element analysis, the microstructural feature that promote failure can be identified with the potential for the manufacturing of the coatings to be improved. One of the challenges of this approach lies in that the manufacture of the beams is found to be more difficult in APS-YSZ than in homogeneous materials such as silicon due to changes in the milling or sputtering rate of the ion beam. It has been shown elsewhere that the complex local morphology leads to a varied milling rate resulting in a significant non-uniformity at the base [8, 9].

5. Conclusions

It may be concluded from this micro-scale investigation that: (i) The diametral compression of small disc specimens provides a useful tool for examining crack formation in quasi-brittle materials such as polygranular reactor core graphite, particularly when supported by focused ion beam milling and imaging. (ii) Micro-cracks in virgin PGA graphite have been confirmed to precede macro-crack formation. The micro-cracking accommodates the non-linearity in the load-displacement curves prior to the peak load. Such cracks have been observed at loads which are as low as 30% of the peak load. (iii) Micro-cantilever testing in APS-YSZ was found to produce comparable mechanical properties and fracture toughness with conventional macro-scale testing. This demonstrates that more insights into the fracture mechanics can be provided by the micro-scale testing.

Acknowledgement

References

[1] E. Schlangen and E. J. Garboczi, Fracture simulations of concrete using lattice models: Computational aspects, Eng. Fract. Mech., 57 (1997) 319-332.
[2] A. Hodgkins, T. J. Marrow, M. R. Wootton, R. Moskovic and P. E. J. Flewitt, Fracture behaviour of radiolytically oxidised reactor core graphites: a view, Mater. Sci. Technol., 26 (2010) 899-907.
[3] A. Hodgkins, T.J. Marrow, P. Mummery, B. Marsden and A. Fok, X-Ray tomography observation of crack propagation in nuclear graphite, Mater. Sci. Technol., 22 (2006) 1045-0151.
[4] P. J. Heard, M. R. Wootton, R. Moskovic and P. E. J. Flewitt, Crack initiation and propagation in pile grade A (PGA) reactor core graphite under a range of loading conditions, J. Nucl. Mater., 401 (2010) 71-77.
[5] P. J. Heard, M. R. Wootton, R. Moskovic and P. E. J. Flewitt, Deformation and fracture of irradiated polygranular pile grade A reactor core graphite, J. Nucl. Mater., 418 (2011) 223-232.
[6] D Liu and P. E. J. Flewitt, The measurement of mechanical properties of thermal barrier coatings by micro-cantilever tests, Key. Eng. Mat., 525-526 (2013) 13-16.
[7] D. Liu, The role of thermal exposure and substrate curvature on the residual stresses and mechanical properties in environmental and thermal barrier coating systems, PhD thesis, University of Bristol, 2012.
[8] J. E. Darnbrough, S Mahalingam and P. E. J. Flewitt, Micro-scale cantilever testing of linear elastic and elastic-plastic materials, Key. Eng. Mat., 525-526 (2013) 57-60.
[9] D. Liu and P. E. J. Flewitt, The Measurement of Mechanical Properties of Thermal Barrier Coatings by Micro-cantilever Tests Key Engineering Materials, Key. Eng. Mat. (2012) 13-16.
[10] K. W. Schlichting, N. P. Padture, E. H. Jordan and M. Gell, Failure modes in plasma-sprayed thermal barrier coatings, Mater. Sci. Eng. A-Struct., 342 (2003) 120-130.
[11] E. Rybicki, J. Shadley, Y. Xiong and D. J. Greving, A Cantilever Beam Method for Evaluating Young's Modulus and Poisson's Ratio of Thermal Spray Coatings, J. Therm. Spray. Tech., 4 (1995) 377-383.
[12] J. A. Thompson and T. W. Clyne, The Effect of Heat Treatment on the Stiffness of Zirconia Top Coats in Plasma-Sprayed TBCs, Acta. Mater., 49 (2001) 1565-1575.
[13] F. Tang and J. M. Schoenung, Evolution of Young's modulus of air plasma sprayed yttria-stabilized zirconia in thermally cycled thermal barrier coatings, Scripta Mater., 54 (2006) 1587-1592.
[14] A. Rabiei and A. G. Evans, Failure mechanisms associated with the thermally grown oxide in plasma-sprayed thermal barrier coatings, Acta. Mater., 48 (2000) 3963-3976.
[15] Y. Yamazaki, S. I. Kuga and T. Yoshida, Evaluation of interfacial strength by a instrumented indentation method and its application to an actual TBC vane, Acta Metall. Sin. (Engl. Lett.), 24 (2011) 109-117.
[16] D. Di Maio and S. G. Roberts, Measuring fracture toughness of coatings using focused-ion-beam-machined microbeams, J. Mater. Res. , 20 (2005) 299-302.